

Theory and simulation of resonant absorption in a hot plasma*

D. W. Forslund, J. M. Kindel, Kenneth Lee, E. L. Lindman, and R. L. Morse

University of California, Los Alamos Scientific Laboratory, Los Alamos, New Mexico 87544

(Received 12 June 1974)

A detailed theoretical and simulation study of resonant absorption in a hot plasma is presented which isolates the behavior of the plasma for times short compared to an ion response time. The extent to which an electron fluid model can describe the absorption process in the kinetic regime is discussed. At high intensities the absorbed energy is observed to be deposited in a suprathermal tail of electrons whose energy varies approximately as the square root of the incident power. The density profile modification due to the ion response to the ponderomotive force is also discussed.

When an electromagnetic wave is obliquely incident on an inhomogeneous plasma and polarized in the plane of incidence, it is well known that it can be absorbed resonantly by linear mode conversion into an electron plasma wave.¹⁻⁷ This process, known as resonant absorption, has important implications for laser target experiments and microwave laboratory experiments.⁸ Most theoretical work has been done for a cold plasma,^{2,4-7} while warm-plasma calculations have been either incomplete³ or incorrect.¹

For gradient lengths long compared to the wavelength of light or $k_0 L \gg 1$ (where k_0 is the incident free-space wave number and L is the density scale length), computer simulations in a hot plasma with fixed ions show that the absorption coefficient is virtually unmodified from the cold-electron case. Theoretical calculations based on a fluid description which agree with these computer simulations indicate that the absorption coefficient is virtually unmodified for temperatures up to 100 keV. At low intensities these theoretical calculations predict the field structures seen in simulations, while at high intensities a nonlinear dissipation must be added to obtain agreement. This nonlinear dissipation is required at high intensities to account for the acceleration towards the low-density region of the plasma of a small number of electrons to very high energies.

To describe resonant absorption in a hot plasma, we combine the linearized electron-momentum equation with Maxwell's equations. An adiabatic pressure law is assumed for the high-frequency electron motion, ion motion is neglected, and the fields are assumed to vary as $e^{i\omega t}$:

$$\begin{aligned} \nabla \cdot \vec{E} &= -4\pi en_1, & \nabla \times \vec{E} &= i(\omega/c)\vec{B}, \\ \nabla \times \vec{B} &= (4\pi/c)\vec{J} - (i\omega/c)\vec{E}, \\ \vec{J} &= \frac{e^2 in_0 \vec{E}}{m(\omega + i\nu)} + \frac{ieT_e}{m(\omega + i\nu_L)} \left(\gamma \nabla n_1 - n_1 \frac{\nabla n_0}{n_0} \right), \end{aligned} \tag{1}$$

where n_0 is the background plasma density; T_e , m , and e are the electron's temperature, mass,

and charge, respectively; c is the velocity of light; and γ is the usual ratio of specific heats and is chosen equal to 3. In factoring the damping in the electron-momentum equation a different damping rate appears in the electric field term than in the electron pressure term. The significance of this phenomenological damping is discussed below. Combining these equations we obtain the general steady-state wave equation for \vec{E} :

$$\begin{aligned} -c^2 \nabla^2 \vec{E} + c^2 \nabla (\nabla \cdot \vec{E}) + \frac{\omega_p^2}{1 + i\nu/\omega} \vec{E} - \omega^2 \vec{E} \\ - \frac{T_e}{m[1 + i\nu_L/\omega]} \left(\gamma \nabla (\nabla \cdot \vec{E}) - \nabla \cdot \vec{E} \frac{\nabla n_0}{n_0} \right) = 0, \end{aligned} \tag{2}$$

where $\omega_p^2 = 4\pi n_0 e^2/m$. In particular, we consider the case of a slab of plasma with $n_0 = n_0(x)$ only and the electromagnetic wave obliquely incident on this slab, with the electric field polarized in the plane of incidence, the x - y plane. The y dependence of the field is assumed to be periodic in y and of the form $e^{ik_y y}$. The coupled equations for E_x and E_y are solved numerically by a standard Gaussian elimination procedure for coupled second-order complex linear differential equations⁹ with arbitrary outgoing wave-boundary conditions.

The use of the phenomenological damping rate ν_L mentioned above permits large damping of the electrostatic component of the wave without altering the electromagnetic component. Comparison with computer simulation results shows that the exact form of ν_L is not very important at low intensity as long as it is sufficiently large to damp the plasma wave in the underdense region, in order to prevent plasma wave reflection from the underdense region back to the generation region. At high intensities simulations show that the electric field accelerates electrons locally to high energy, with relatively little energy going into the plasma wave. This effect can be modeled in the fluid equations by an appropriate local increase in ν_L .

It is useful to consider the size of ν and ν_L re-

quired to model the kinetic effects in this fluid model. For weak damping in the WKB approximation the spatial damping rate on a plasma wave with the above form for the damping is

$$\frac{\text{Im}k}{\text{Re}k} = \frac{1}{2} \frac{\omega_p^2}{\omega^2 - \omega_p^2} \frac{\nu}{\omega} + \frac{1}{2} \frac{\nu_L}{\omega}. \quad (3)$$

Thus, very close to the turning point ($1 - \omega_p^2/\omega^2 \ll 1$) ν_L is much less effective in damping the plasma wave than is ν , which is equivalent to the usual collision frequency in that regime. An extra factor of $1/\epsilon = \omega^2/(\omega^2 - \omega_p^2) \approx \omega^2/\gamma k^2 v_e^2$, where $v_e^2 = T_e/m$, is then needed in ν_L to model electron Landau damping:

$$(\nu_L/\omega) = (\frac{1}{8}\pi)^{1/2} (\gamma/\epsilon)^{5/2} e^{-\gamma/\epsilon}. \quad (4)$$

It has been shown³ that the convection of plasma waves away from the turning point is equivalent to an effective collision frequency of $\nu_{\text{eff}}/\omega \approx 1/k_{\text{min}}L = (\nu_e/\omega L)^{2/3}$ in terms of loss of energy from the region. If the plasma wave were to dissipate all its energy locally at the turning point, as it must in a cold plasma, we would have $\text{Im}k/\text{Re}k \sim 1$. This requires a $\nu/\omega \sim 1/k_{\text{min}}L$ or $\nu_L/\omega \sim 1$. Thus, in the simulations described below, if local deposition of energy in hot electrons is important, we would expect to find $\text{Im}k \sim \text{Re}k$ and would require $\nu_L/\omega \sim 1$ in order to model this effect with the fluid equations.

Equation (2) has been solved for a range of angles, density gradient lengths, and electron temperatures. For linear density profiles Fig. 1 contains a plot of the absorption coefficient as a function of $(k_0L)^{2/3} \sin^2 \theta$ for $k_0L \gg 1$ (L is the distance from zero to critical density where $\omega = \omega_p$ and θ is the angle of incidence) for two electron temperatures $T_e/mc^2 = 0.005$ and 0.1 , i.e., 2.5 and 50 keV, respectively. Even over this range of temperature the peak absorption is still nearly 50%.

The case $T_e/mc^2 = 0.005$ is virtually identical to the results for a cold plasma. The analytic solution of Piliya¹ is the dashed curve shown for comparison. The points with error bars are the absorption coefficients measured with the computer simulation code described below.

The equation for the longitudinal component of \vec{E} , E_x , has been shown by Piliya¹ to have approximate Airy-function solutions near the plasma-wave turning point in a linear density profile. Numerical solutions of Eq. (2) show that near the turning point $E_x \propto (k_0L)^{1/6} T_e^{-1/3}$ and $n_1 \propto (k_0L)^{-1/6} \times T_e^{-2/3}$ at the optimum angle for absorption $(k_0L)^{2/3} \sin^2 \theta \approx 0.5$, consistent with these Airy-function solutions. For a linear density profile with $k_0L = 12.5$, numerical solutions for n_1 , E_x , and B_z are shown in Fig. 2. A light wave with amplitude $e|E|/m\omega c \equiv v_0/c = 0.015$ is launched at an angle $\sin \theta = 0.4$ at the left boundary into the plasma, which has an electron temperature $T_e/mc^2 = 0.00125$, i.e., 625 eV. Strong damping is put on the plasma wave to prevent significant propagation away from its turning point, which is at $x = 16.25c/\omega$. Note the factor-of-8 enhancement of the E_x field as the light wave is converted into a plasma wave. Comparisons are also made in the figure to simulations discussed below.

A two-dimensional (2D) electromagnetic PIC (particle-in-cell) code WAVE (a version of the code used to do the first 2D cold-plasma simulations of resonant absorption discussed in Ref. 2) which is periodic in the y direction and aperiodic in the x direction has been used to carry out extensive studies of the linear and nonlinear behavior of resonant absorption without having to make the fluid approximation discussed above. The agreement between these kinetic simulations and the fluid linear theory is surprisingly good, even for nonlinear power levels, i.e., power levels where the incident field

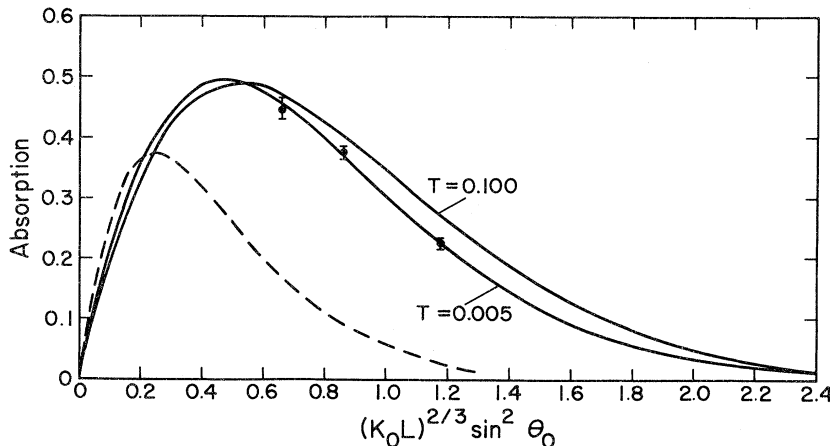


FIG. 1. Absorption as a function of $(K_0L)^{2/3} \sin^2 \theta$ given by numerical solutions of Eqs. (1) for two temperatures $T \equiv T_e/mc^2 = 0.005$ and 0.1 and $k_0L \gg 1$; $\theta_0 = \sin^{-1}(k_y/k_0)$ is the angle of incidence. Simulation results are shown for $k_0L = 12.5$ at three angles. The dashed line is a curve calculated by Piliya (Ref. 1).

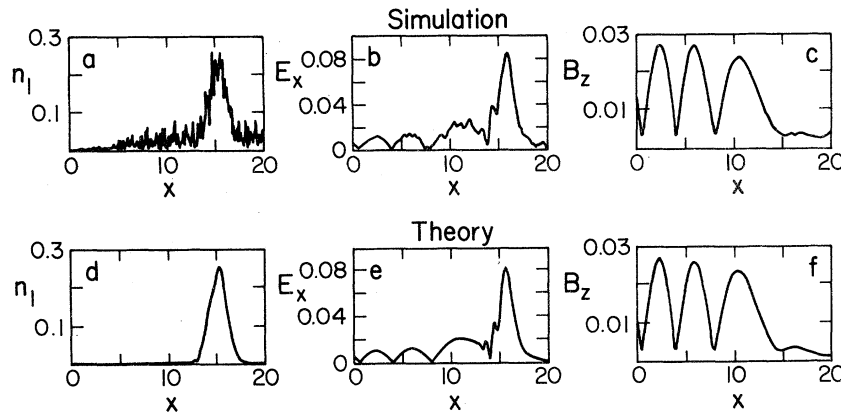


FIG. 2. Simulation [(a)–(c)] and theoretical [(d)–(f)] results comparing n_1 , the perturbed electron density in units of the critical density; E_x , the electric field along the density gradient direction; and B_z , the wave magnetic field. The fields are expressed in the units $mc\omega/e$. The electron temperature is $T_e/mc^2 = 0.00125$, i.e., 625 eV.

E is so large as to predict $n_1/n_0 \sim O(1)$. The absorption coefficient and the size and spatial dependence of B_z agree exactly with theory, independent of ν_L , whereas n_1 and E_x agree within a few percent of theoretical predictions if ν_L is enhanced above the Landau value near the plasma-wave turning point.

For diagnostic purposes the various field components as well as the electron density are Fourier analyzed in the y direction, and the resulting amplitudes for each y mode are plotted as a function of x . The incident light wave has the y component of its wavelength equal to the size of the box in y . Hence it and the plasma wave it linearly excites appear in the fundamental mode in y . Such a diagnostic has two advantages. First, it allows the separation of the perturbed plasma-wave density from the nonuniform equilibrium. Second, the averaging process inherent in the Fourier analysis reduces the noise level by about an order of magnitude over that of a line plot versus x at a fixed y .

For comparison with the linear fluid theory we show the magnitude of n_1 , E_x , and B_z in Figs. 2(a)–2(c). Note that n_1 and E_x peak near the critical density at $x = 16.25c/\omega$, while from Fig. 2(c) we see that B_z tunnels in from the electromagnetic turning point at $14.25c/\omega$ ($\omega = \omega_p \sec \theta$), coupling energy into the electrostatic peaks. Note also that the plasma-wave amplitude as seen in E_x decays in just a few wavelengths implying, $\text{Im}k/\text{Re}k \lesssim 1$. Thus we expect that the plasma-wave damping ν_L/ω must be large near its turning point. In fact, to obtain the agreement shown in Fig. 2 ν_L/ω was chosen equal to 0.09 at the critical density, with a rapid spatial drop away from that point. The field amplitudes, however, are not sensitive to the form of the spatial dependence of ν_L .

If one considers the v_x - x component of electron phase space over a narrow band in y (a fraction

of a wavelength in y), one can determine the source of plasma wave damping. A small fraction of the electrons are accelerated by the localized electrostatic field toward the lower-density region at

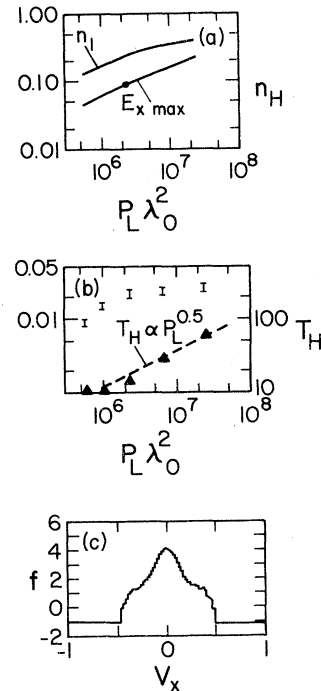


FIG. 3. (a) Simulation results showing the maximum value of n_1 and E_x as a function of power, $P_L \lambda_0^2$ (watts) $= 10^{10} v_0^2 / c^2$. Theoretical results lie along these curves if a nonlinear damping ν_L is used. (b) Fractional density of hot electrons n_H/n_c and the hot electron temperature T_H (triangles) as a function of power. The background temperature in all cases is $T_e = 625$ eV. (c) Electron distribution function along the density gradient direction for $v_0/c = 0.015$; v_x is in units of c . A gradient of $k_0 L = 12.5$ was used.

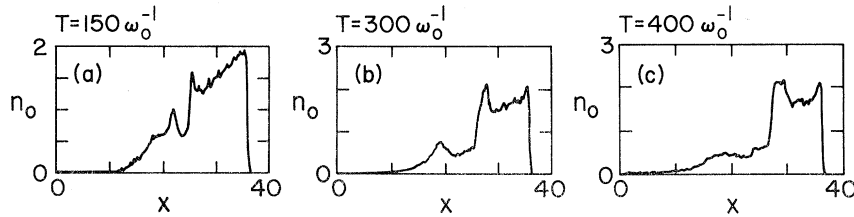


FIG. 4. (a), (b), and (c): A typical high-power simulation showing the ion density profile at three times for the simulation parameters $v_0/c=0.1$, $v_e/c=0.07$, $k_0L=12.5$, and $M/m=100$.

velocities which are a large fraction of the speed of light. These electrons are accelerated to this velocity in only a single transit of the structure, giving rise to substantial dissipation of the plasma wave.

The dependence of the peak values of n_1/n_0 and $eE_x/m\omega c$ as a function of incident laser power P_L is shown in Fig. 3(a). Note that at low powers both n_1 and E_x vary directly with the square root of P_L according to linear theory. At higher power, e.g., $v_0/c \geq 0.015$ or 2×10^{12} W/cm² for 10- μ m light, it is clear that the maximum of n_1 increases much more slowly than $P_L^{1/2}$. This is due to the increased nonlinear damping of the plasma wave, as evidenced by the increased electron heating and by the reduction in the amplitude of the plasma waves radiated from the critical density. In fact, for the fluid theory to agree at higher powers $v_L \sim \omega$ is required, since $\text{Im}k/\text{Re}k \sim 1$. Clearly, at this point it is not useful to call the highly localized electrostatic perturbation a plasma wave. At still higher powers the effect of the electron pressure is negligible and one obtains the cold-plasma picture described in Ref. 2. The transition to the regime of strong damping is determined by comparing the maximum value of E_x determined by the breaking condition of Ref. 2 with that determined by the linear convective loss of the plasma wave. The threshold is then $v_0/v_e > (k_0L)^{1/2}(v_e/\omega L)^{1/3}$.

To give some idea of the large amount of electron heating which resonant absorption can cause, we plot in Fig. 3(b) the fractional number of hot electrons and their corresponding energy T_H as a function of incident laser power. Although the hot electrons do not necessarily make a simple Maxwellian velocity tail, T_H is a useful parameter to give some idea of the energy in the tail. For the chosen gradient length we find T_H (keV) $\approx 0.01\lambda_0$ (cm) $[P_L(\omega/\text{cm}^2)]^{1/2}$, a scaling predicted in Ref. 2. Almost all of the absorbed energy goes into producing these electron tails.

For completeness, Fig. 3(c) shows a typical electron velocity distribution of v_x for $v_0/c=0.015$. Velocities are in units of the speed of light. Initially electrons are accelerated in x by the local electrostatic field towards lower-density regions at velocities which are a large fraction of the speed

of light. These electrons reflect off of the low-density electron sheath and return to higher densities. They are then replaced by thermal electrons when they strike the right boundary of the simulation box—simulating interaction with a region of high-density cold plasma. After a time $T \approx 300\omega^{-1}$, the steady-state distribution is as shown in Fig. 3(c).

We expect that the excited electron plasma wave should itself be parametrically unstable in cases where the ions are mobile. This has already been considered theoretically.¹⁰ Simulations show that this effect may reduce the extreme electron energies by stochastically heating the electrons rather than coherently accelerating them. Simulations with mobile ions also show rather dramatic profile modification, wherein the initially linear density ramp begins to develop a density depression near the critical density. At higher power and late times a flat density shelf below the critical density and a steepening of the profile at the critical density develop.¹¹ Figures 4(a), 4(b), and 4(c) show what happens to the ion density profile as a function of time for a typical high-power simulation. Particular parameters are $v_0/c=0.1$, $T_e/mc^2=0.005$, ion-to-electron-mass ratio $M/m=100$, and $\sin\theta=0.4$. The initial density profile rises from zero density to twice critical in a distance $25c/\omega$, i.e., $k_0L=12.5$. We see that after resonance absorption begins ($T \approx 100\omega^{-1}$) the ponderomotive force makes a density hole around critical density, while at later times, as the ions blow off, a density shelf forms. At this time the absorption rises significantly. This will be discussed further in a subsequent paper.¹²

To summarize, we find that a simple set of two coupled second-order differential equations can accurately model the behavior of resonant absorption in a hot plasma. Furthermore, we can solve these equations for a wider class of density profiles than can be done economically by numerical simulations. For example, they can be interfaced with a hydrodynamics code to determine long-time absorption and profile-modification effects. Details of how this can be done will be given in another paper.¹²

*Work performed under the auspices of the United States Atomic Energy Commission.

- ¹A. D. Piliya, Zh. Tekh. Fiz. 36, 818 (1966) [Sov. Phys.—Tech. Phys. 11, 609 (1966)].
- ²J. P. Freidberg, R. W. Mitchell, R. L. Morse, and L. I. Rudsinski, Phys. Rev. Lett. 28, 795 (1972).
- ³N. G. Denisov, Zh. Eksp. Teor. Fiz. 31, 609 (1956) [Sov. Phys.—JETP 4, 544 (1957)]; V. B. Gil'denburg, Zh. Eksp. Teor. Fiz. 45, 1978 (1963) [Sov. Phys.—JETP 18, 1359 (1964)].
- ⁴R. P. Godwin, Phys. Rev. Lett. 28, 85 (1972); M. M. Mueller, Phys. Rev. Lett. 30, 582 (1973).
- ⁵V. L. Ginzburg, *Propagation of Electromagnetic Waves in Plasmas* (Pergamon, New York, 1970), p. 260ff.
- ⁶K. G. Budden, *Radio Waves in the Ionosphere* (Cambridge U. P., Cambridge, England, 1961), p. 348ff; P. Hirsch and J. Shmoys, Radio Sci. 690, 521 (1965); A. V. Vinogradov and V. V. Pustavalov, Zh. Eksp. Teor. Fiz. Pis'ma Red. 13, 317 (1971) [JETP Lett. 13, 226 (1971)].
- ⁷R. B. White and F. F. Chen, Plasma Phys. 16, 565 (1974).
- ⁸R. L. Stenzel, A. Y. Wong, and H. C. Kim, Phys. Rev. Lett. 32, 654 (1974).
- ⁹R. D. Richtmyer and K. W. Morton, *Difference Methods for Initial Value Problems* (Interscience, New York, 1967), p. 199ff.
- ¹⁰R. B. White, C. S. Liu, and M. N. Rosenbluth, Phys. Rev. Lett. 31, 520 (1973).
- ¹¹D. W. Forslund, J. M. Kindel, and E. L. Lindman, Progress Report of the Laser Program at LASL, July 1–December 31, 1973 (unpublished), p. 67, H. C. Kim, R. L. Stenzel, and A. Y. Wong, Phys. Rev. Lett. 33, 886 (1974); V. B. Gil'denburg, Zh. Eksp. Teor. Fiz. 46, 2156 (1964) [Sov. Phys.—JETP 19, 1456 (1964)]; K. G. Estabrook, E. J. Valeo, and W. L. Kruer, Lawrence Livermore Laboratory Report on Two-Dimensional Relativistic Simulations of Resonance Absorption, May, 1974 (unpublished).
- ¹²D. W. Forslund, J. M. Kindel, Kenneth Lee, and E. L. Lindman, LASL Report No. LA-UP-74-1636, 1974 (unpublished).